OPTIMAL CONTROL OF MAGNETIC FIELDS IN FLOW MEASUREMENT *

SERGE NICAISE†, SIMON STINGELIN‡, AND FREDI TRÖLTZSCH§

Dedicated to the 65th birthday of Prof Jürgen Sprekels

Abstract. Optimal control problems are considered for transient magnetization processes arising from electromagnetic flow measurement. The magnetic fields are generated by an induction coil and are defined in 3D spatial domains that include electrically conducting and nonconducting regions. Taking the electrical voltage in the coil as control, the state equation for the magnetic field and the electrical current generated in the induction coil is a system of integro-differential evolution Maxwell equations. The aim of the control is a fast transition of the magnetic field in the conducting region from an initial polarization to the opposite one. First-order necessary optimality condition and numerical methods of projected gradient type are discussed for associated optimal control problems. To deal with the extremely long computing times for this problem, model reduction by standard proper orthogonal decomposition is applied. Numerical tests are shown for a simplified geometry and for a 3D industrial application.

AMS subject classification. 35K65, 35B37, 78A25

Key words. Evolution Maxwell equations, integro-differential equation, degenerate parabolic equation, vector potential formulation, induction law, optimal control, adjoint equation, numerical solution, model reduction, proper orthogonal decomposition

1. Introduction. In this paper, we extend our investigations in [20] on optimal magnetization problems arising from industrial applications in flow measurement. The main problem can be described as follows:

An electrically conducting fluid moves through a tube of metal. To determine its velocity, an electrical potential is measured at selected points inside the tube. This volume flow measurement is performed differentially with a pulsed magnetic field to suppress noise and offset voltages as efficiently as possible, see Fig. 1.1. If the magnetic field changes in time, then an electrical potential is measured although the velocity of the fluid did not change. The measurement would indicate a flow that does not exist. Therefore, the aim of the control is to reach a steady state of the magnetic induction in shortest time. By controlling the electrical voltage in the induction coils, magnetic fields should be switched very fast from a given steady magnetic field to the one with opposite polarization.

We model the magnetization process by a linear parabolic-elliptic evolution Maxwell system that is complemented by an integro-differential equation accounting for the induction law in the coils. Our quantity of interest is the magnetic induction B in the tube. Following our method of [20], we express B by a vector potential A and investigate A rather than B; we have $B = \operatorname{curl} A$.

As optimization criterion, we apply two different type of quadratic tracking functionals. In the first that was also considered in [20], we minimize the L^2-distance of the vector potential A to a desired vector potential. In the second, we aim at minimizing the L^2-distance of the magnetic

*This work was supported by Endress+Hauser Flowtec AG Reinach (Switzerland).

†LAMAV and FR CNRS 2956, Université de Valenciennes et du Hainaut Cambrésis, Institut des Sciences et Techniques of Valenciennes, F-59313 - Valenciennes Cedex 9 France (Serge.Nicaise@univ-valenciennes.fr).

‡Endress+Hauser Flowtec AG, Kägenstrasse 7, CH-4157 Reinach BL, Switzerland (simon.stingelin@flowtec.endress.com)

§Institut für Mathematik, Technische Universität Berlin, D-10623 Berlin, Germany (troeltzsch@math.tu-berlin.de).

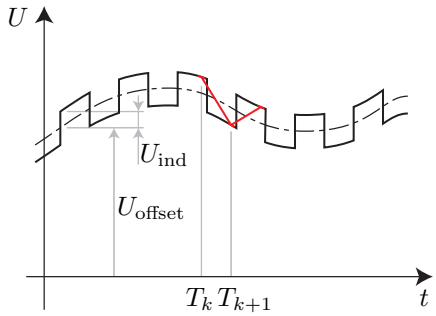

FIG. 1.1. *Differential volume flow measurement with pulsed magnetic field*

induction B to a desired one. Eventually, this leads to the minimization of the distance of curl A to the desired induction field, a problem that is more demanding but yields better results for an industrial configuration. This is the first novelty of our paper that is mainly addressed from a numerical point of view.

Another new issue is the application of model order reduction to the state equations. In [20] we report on very long computing times for the full problem that is discretized by a finite element method in space and the implicit Euler method in time. For a realistic industrial setting, any solution of the state equation typically needed more than 5 hours, too much for a practicable implementation of numerical optimization methods. Therefore, we applied proper orthogonal decomposition (POD) to drastically decrease the computing times. In this paper, we report on our experience with POD.

Our paper is another contribution to the optimal control theory related to Maxwell equations, a field that became quite active in the last years. Let us give a brief account on some related references. In the optimal control of processes of magneto-hydrodynamics (MHD), the control system includes Maxwell equations coupled with equations accounting for fluid flow and/or heat conduction. We mention [5], [7], [8], [9], [12], or [13] and further references cited therein. In these papers, steady state or time-harmonic Maxwell equations are used, while the Navier-Stokes equations for fluid flow are time variant.

The time harmonic setting is also used in [6], [11], [16], [19], [25], [26]. Moreover, we refer to the recent PhD thesis [2], where time optimal magnetization problems are studied in academic 3D geometries.

Concentrating on the magnetic field, [15] and [16] deal with the optimal control of magnetic fields in a time-harmonic setting of the Maxwell equations. The last two papers are closer to our model than the problems of control in MHD. In contrast to the references cited above, our problems of optimal magnetization are modeled by evolution Maxwell equations of degenerate parabolic type. In the mathematical analysis, we are able to invoke results of [21] on existence and uniqueness for the state equations. We also mention the contribution [22] on the application of POD to the optimal control of Maxwell equations.

2. Model and industrial background.

2.1. Evolution Maxwell equation.

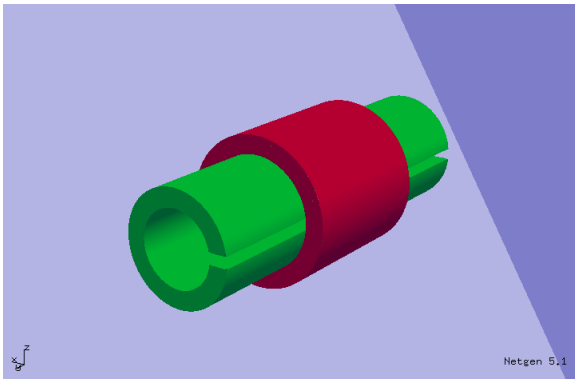

FIG. 2.1. *A tube with coil and a slit*

Geometrical settings. We consider the magnetization processes in a bounded spatial domain $\Omega \subset \mathbb{R}^3$ that is our "holdall domain" for the whole setting. In our test examples, Ω is a sufficiently big cube. This domain Ω is the union of the electrically conducting domain Ω_1 and the electrically nonconducting domain Ω_2, more precisely

$$\bar{\Omega} = \bar{\Omega}_1 \cup \bar{\Omega}_2.$$

By $\Gamma := \bar{\Omega}_1 \cap \bar{\Omega}_2$ the interface between the conducting and nonconducting region is denoted and by $\nu : \partial\Omega \to \mathbb{R}^3$ the vector field of the outer unit normal on $\partial\Omega$.

Moreover, another open set $\Omega_c \subset \Omega_2$ is given that stands for region of the coils. We shall specify the concrete assumptions on the associated geometry below.

We rely on the following geometric assumptions: The sets Ω, Ω_1, Ω_2, and Ω_c are (open) bounded Lipschitz domains such that $\bar{\Omega}_1 \subset \Omega$ (i.e. Ω_1 is strictly included in Ω), Ω_2 has exactly one hole formed by $\bar{\Omega}_1$ and that the boundary $\partial\Omega_2$ is composed of two connected components. We have $\Omega_c \subset \Omega_2$; notice that the coil region Ω_c is modeled as part of the nonconducting region.

Let us present two examples of geometries, where these assumption are satisfied. In both examples the holdall domain $\Omega \subset \mathbb{R}^3$ is an open cube that contains the union of the conducting region with the coil region.

(i) Academic geometry. We used this geometry for many computational tests. It is the configuration of a tube surrounded by a coil, see Fig. 2.1. In the figure, the coil is painted in red, the core in green, and the remaining nonconducting part is blue in the picture. Precisely, the figure shows a tube with a slit, the configuration without slit is obtained by an obvious modification.

For the tube without slit, Ω_1 and Ω_2 are defined as follows: The tube Ω_{tb} is given by

$$\Omega_{tb} = \{x \in \mathbb{R}^3 \,:\, 0 < r_1 < x_1^2 + x_2^2 < r_2,\ z_1 < x_3 < z_2\},$$

while the induction coil occupies the domain

$$\Omega_c = \{x \in \mathbb{R}^3 \,:\, 0 < r_2 < x_1^2 + x_2^2 < r_3,\ c_1 < x_3 < c_2\}.$$

In this setting, $r_3 > r_2$ and $z_1 \le c_1 < c_2 \le z_2$ are given real numbers.

EXAMPLE 1. *In our numerical tests with simplified geometry, the holdall domain Ω is a cube of side length $0.2m$ centered at the origin. The tube is taken parallel to one of the sides, centered in the cube. For the tube, we selected the following data:*

$$r_1 = 0.01\,m, \quad r_2 = 0.015\,m, \quad z_1 = -0.05\,m, \quad z_2 = 0.05\,m,$$

and

$$r_3 = 0.02\,m, \quad c_1 = -0.02\,m, \quad c_2 = 0.02\,m.$$

In the configuration with slit shown in Fig. 2.1, the thickness of the slit is $0.003\,m$.

The tube with coil is the union $\bar{\Omega}_{tb} \cup \bar{\Omega}_c$. In our modeling, Ω_c is part of the nonconducting domain so that we have

$$\Omega_1 = \Omega_{tb}$$

as conducting domain and

$$\Omega_2 = \Omega \setminus \bar{\Omega}_{tb}$$

as nonconducting one.

(ii) Simplified industrial geometry. As real world example, we considered an industrial sensor of nominal diameter 50 mm for flow measurement (DN 50 sensor) produced by the Endress+Hauser Flowtec Company, see the left side of the Fig. 2.2. Here, one quarter of the setting is extracted. The coil, painted in yellow, is located on top of the tube. It is carried by some magnetic system that is colored in grey. The fluid flows through the horizontal tube that is painted in blue. Only the magnetic system is modeled as electrical conductor, while the other parts are considered as non-conducting. Notice that the magnetic system is simply connected, hence the nonconducting region has a simply connected hole.

In the right side of Figure 2.2, real industrial sensors of different size are shown. Their induction coils are located on top of the tube.

A basic version of the state equation. Our main quantity of interest, the magnetic induction $B : \bar{\Omega} \to \mathbb{R}^3$, is assumed to be divergence free. Therefore, B can be represented by a vector potential $A : \bar{\Omega} \to \mathbb{R}^3$, namely $B := \operatorname{curl} A$. Inserting A in the Maxwell equations and neglecting the very small term $\epsilon\,\partial^2 A/\partial t^2$, we finally arrive at the following eddy current formulation of the Maxwell equations,

$$\left\{ \begin{array}{rcll} \sigma(x)\dfrac{\partial A}{\partial t}(x,t) + \operatorname{curl}\mu^{-1}\operatorname{curl} A(x,t) &=& F(x,t) \quad \text{in} & \Omega \times (0,T) \\ A(x,t) \times \nu &=& 0 \quad \text{on} & \partial\Omega \times (0,T) \\ A(x,0) &=& A_0(x) \quad \text{in} & \Omega_1. \end{array} \right. \tag{2.1}$$

We will specify $F : \Omega \times (0,T) \to \mathbb{R}^3$ and $A_0 : \Omega_1 \to \mathbb{R}^3$ later. The *electrical conductivity* $\sigma : \Omega \to \mathbb{R}$ is given with some constant $\sigma_0 > 0$ by

$$\sigma(x) := \left\{ \begin{array}{ll} \sigma_0 & \text{in} \quad \Omega_1 \\ 0 & \text{in} \quad \Omega_2. \end{array} \right.$$

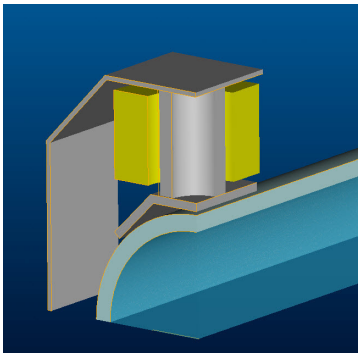


FIG. 2.2. *Scheme of a tube with industrial sensor DN50 (left) and industrial sensors for tubes of large and small size (right); courtesy of Endress+Hauser Flowtec AG*

The *magnetic permeability* $\mu : \Omega \to \mathbb{R}$ is assumed to be bounded and measurable and to obey

$$\mu(x) \geq \mu_0 > 0 \quad \text{for a.a. } x \in \Omega.$$

As in (2.1), the partial differential equation reduces to $\operatorname{curl} \mu^{-1} \operatorname{curl} A = F$ in Ω_2, a gauge condition has to be imposed on A. We comment on this after Lemma 3.1 below.

As we have mentioned above, we model the induction coil as part of the nonconducting region. The reason is that we do not invoke the Maxwell equations for computing the electrical current in the windings of the coil. An induction coil contains a wire that forms many windings around the core. It is clear that a cross section through these windings has a complicated geometry. The numerical computation of the electrical current in the windings via Maxwell's equations is a fairly hopeless task.

Therefore, we adopt the following widely used idea: First, we derive a simpler law for the relation between electrical current and electrical voltage. Next, having a good approximation of the amplitude of the electrical current, we extend this to all points x of the induction coil by some process of homogenization: For the current density I_c induced in the coil, we use the ansatz

$$I_c(x,t) = E(x)\, i(t),$$

where the vector E defines the direction of the electrical current in the point x and $i(t)$ is the amplitude of the current density in a single winding at time t. Here, E is defined by

$$E(x_1,x_2,x_3) = \begin{cases} \dfrac{N_c}{|\omega_c|\sqrt{x_1^2+x_2^2}} \begin{bmatrix} -x_2 \\ x_1 \\ 0 \end{bmatrix} & \text{in } \Omega_c \\ 0 & \text{else,} \end{cases} \tag{2.2}$$

where N_c is the number of windings and $|\omega_c|$ denotes the area of the cross section of a rectangular cut through the coil that is seen in Fig. 2.3. Note that E is divergence free in the whole domain Ω. Given the electrical current i, the vector potential A can be determined as solution of the

parabolic-elliptic evolution Maxwell equations

$$\left\{\begin{array}{rcll} \sigma_0 \dfrac{\partial A}{\partial t}(x,t) + \operatorname{curl} \mu^{-1} \operatorname{curl} A(x,t) &=& 0 & \text{in} \quad \Omega_1 \times (0,T) \\ \operatorname{curl} \mu^{-1} \operatorname{curl} A(x,t) &=& E(x)\, i(t) & \text{in} \quad \Omega_2 \times (0,T) \\ A(x,t) \times \nu &=& 0 & \text{on} \quad \partial\Omega \times (0,T) \\ A(x,0) &=& A_0(x) & \text{in} \quad \Omega_1. \end{array}\right. \tag{2.3}$$

It remains to determine the amplitude $i(t)$. Let $u(t)$ denote the electrical voltage imposed on the coil at time t and R_c be the electrical resistance of the wire. Given the voltage, a first idea of determining the electrical current in the wire might be the use of Ohm's law,

$$R_c\, i(t) = u(t),$$

where R_c is the resistance of the wire. However, this would not comply with the induction law in the coil. Instead, we apply the formula

$$\begin{array}{rcll} \displaystyle\int_\Omega \frac{\partial A}{\partial t}(x,t) \cdot E(x)\, dx + R_c\, i(t) &=& u(t), \quad t \in (0,T), \\ i(0) &=& i_0. \end{array} \tag{2.4}$$

Since E was defined to be zero outside the coil Ω_c, the integral above is in fact one on Ω_c.

Let us briefly explain this formula. Thanks to the induction law, it must hold

$$\frac{d}{dt}\Psi(t) + R_c\, i(t) = u(t),$$

where

$$\Psi(t) = \int_{\mathcal{F}_c} B(t) \cdot dS$$

is the total magnetic flux through the area spanned by all windings and $\mathcal{F}_c$ is the surface spanned by the windings of the coil, cf. Fig. 2.3.

Now, we proceed as follows (see also Fig. 2.3 for the definition of $\mathcal{F}_c$ and Ω_c)

$$\begin{aligned} \frac{d}{dt}\Psi(t) &= \int_{\mathcal{F}_c} \frac{\partial B}{\partial t}(t) \cdot dS = \int_{\mathcal{F}_c} \frac{\partial}{\partial t}(\operatorname{curl} A(t)) \cdot dS \\ &= \int_{\mathcal{F}_c} \operatorname{curl} \frac{\partial A}{\partial t}(t) \cdot dS = \oint_{\partial \mathcal{F}_c} \frac{\partial A}{\partial t}(t) \cdot ds \\ &\approx \frac{N_c}{|\omega_c|} \int_{\Omega_c} \frac{\partial A}{\partial t}(t) \cdot w \; dx = \int_{\Omega_c} \frac{\partial A}{\partial t}(t) \cdot E \; dx, \end{aligned}$$

where we used the current direction w with $\operatorname{div} w = 0$ and $|w| = 1$ introduced above, namely

$$w = \frac{1}{\sqrt{x_1^2 + x_2^2}} \begin{bmatrix} -x_2 \\ x_1 \\ 0 \end{bmatrix}.$$

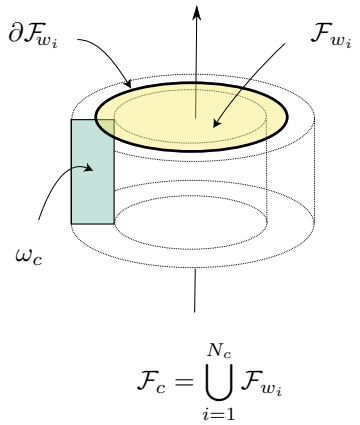

FIG. 2.3. *Total induction and cross sections in the coil*

Now we are able to set up the state equation of our optimal control problem. The only domain with a given source term is the coil domain Ω_c. Complementing the original system by this equation, we arrive at the following integro-differential model as state equation of our optimal control problem:

$$\left\{\begin{aligned}
\sigma_0 \frac{\partial A}{\partial t}(x,t) + \operatorname{curl} \mu^{-1} \operatorname{curl} A(x,t) + \varepsilon\, A(x,t) &= 0 && \text{in} && \Omega_1 \times (0,T) \\
\operatorname{curl} \mu^{-1} \operatorname{curl} A(x,t) + \varepsilon\, A(x,t) &= E(x)\, i(t) && \text{in} && \Omega_2 \times (0,T) \\
A(x,t) \times \nu &= 0 && \text{on} && \partial\Omega \times (0,T) \\
[A(x,t) \times \nu] &= 0 && \text{on} && \Gamma \times (0,T) \\
[\mu^{-1} \operatorname{curl} A(x,t) \times \nu] &= 0 && \text{on} && \Gamma \times (0,T) \\
A(x,0) &= A_0(x) && \text{in} && \Omega_1 \\
\\
\int_\Omega \frac{\partial A}{\partial t}(x,t) \cdot E(x)\, dx + R_c\, i(t) &= u(t) && \text{in} && (0,T) \\
i(0) &= i_0.
\end{aligned}\right. \tag{2.5}$$

Here, $\varepsilon \geq 0$ is introduced as elliptic regularization term that turned out to be very useful in numerical computations, and $[\cdot]$ denotes the jump of a quantity in the brackets through Γ. In what follows, we shall call this system the *full system*.

The analysis of (2.5) is more delicate than that for (2.1) or (2.3) that can be performed along the lines of [4], we also refer to [21]. In a first step, we eliminate the current i by the integro-differential part of (2.5),

$$i(t) = \frac{1}{R_c} \left(u(t) - \int_\Omega \frac{\partial A}{\partial t}(x,t) \cdot E(x)\, dx \right) \tag{2.6}$$

and insert this in the differential part. We get the degenerate parabolic integro-differential equation

$$\begin{cases} \sigma_0 \dfrac{\partial A}{\partial t}(x,t) + \operatorname{curl} \mu^{-1} \operatorname{curl} A(x,t) + \varepsilon\, A(x,t) &= 0 & \text{in} \quad Q_1 \\ \dfrac{1}{R_c} \displaystyle\int_{\Omega_c} \dfrac{\partial A}{\partial t}(\xi,t) \cdot E(\xi)\, d\xi\, E(x) & & \\ \qquad + \operatorname{curl} \mu^{-1} \operatorname{curl} A(x,t) + \varepsilon\, A(x,t) &= \dfrac{1}{R_c} E(x)\, u(t) & \text{in} \quad Q_2 \\ A(x,t) \times \nu &= 0 & \text{on} \quad \Sigma \\ A(x,0) &= A_0(x) & \text{in} \quad \Omega_1, \end{cases} \tag{2.7}$$

where $Q_j := \Omega_j \times (0,T)$, $j = 1, 2$, and $\Sigma := \partial\Omega \times (0,T)$.

By our substitution, we have lost the initial condition $i(0) = i_0$. Moreover, it is not clear if i is continuous so that $i(0)$ is well defined. Therefore, following [21], we take a detour. First, we complete the system (2.7) by the somehow artificial initial condition

$$\int_{\Omega_c} A(x,0) \cdot E(x)\, dx = \alpha_0 \tag{2.8}$$

with some given real number α_0. If i is a continuous function, then we are able to fix α_0 in such a way that the initial condition $i(0) = i_0$ is satisfied. Let us denote this system as the *shortened system*, because i was eliminated from the equations.

Function spaces and weak solutions. Let $\mathcal{O} \subset \mathbb{R}^3$ be a nonempty open domain. We use the standard Sobolev spaces $H(\operatorname{curl}, \mathcal{O})$ and $H(\operatorname{div}, \mathcal{O})$ and the space

$$H(\operatorname{div} = 0, \mathcal{O}) := \{A \in L^2(\mathcal{O})^3 : \operatorname{div} A = 0 \text{ in } \mathcal{O}\},$$

the space of divergence free vector functions equipped with the inner product of $L^2(\mathcal{O})^3$. It is well known that this is a Hilbert space. Moreover, we need the space

$$H_0(\operatorname{curl}, \Omega) := \{A \in L^2(\Omega)^3 : \operatorname{curl} A \in L^2(\Omega)^3 \text{ and } A \times \nu = 0 \text{ on } \partial\Omega\}.$$

As state space for our problem, we define

$$Y(\Omega) := \{A \in H_0(\operatorname{curl}, \Omega) \,:\, \operatorname{div} A_{|\Omega_j} \in L^2(\Omega_i)^3,\ j = 1, 2, \text{ and } \langle A_{|\Omega_2}, \nu \rangle_\Gamma = 0\}.$$

Here, $\langle \cdot\,, \cdot \rangle_\Gamma$ denotes the pairing between $H^{-1/2}(\Gamma)$ and $H^{1/2}(\Gamma)$. Moreover, we define the space V

$$V := \{A \in L^2(\Omega)^3 \,:\, \operatorname{div} A_{|\Omega_1} = 0 \text{ and } \operatorname{div} A_{|\Omega_2} = 0 \text{ and } \langle A_{|\Omega_2}, \nu \rangle_\Gamma = 0\}.$$

These spaces may be defined on the fields of real or complex numbers. Due to our application, the vector potential A is assumed to be real. In the weak formulations of our state equations, the test functions z are taken from the associated complex spaces.

To define the notion of a weak solution of the shortened system, we introduce the following sesquilinear form $a_0 : Y(\Omega) \times Y(\Omega) \to \mathbb{C}$:

$$\begin{aligned} a_0(y,z) = &\int_\Omega \mu^{-1} \operatorname{curl} A \cdot \operatorname{curl} \bar{z} \, + \varepsilon\, A \cdot \bar{z}\, dx \\ &+ e^{i\frac{\pi}{4}} \int_{\Omega_1} \operatorname{div} A_1 \operatorname{div} \bar{z}_1\, dx + e^{i\frac{\pi}{4}} \int_{\Omega_2} \operatorname{div} A_2 \operatorname{div} \bar{z}_2\, dx. \end{aligned} \tag{2.9}$$

In this definition, A_j stands for $A_{|\Omega_j}$, $j = 1, 2$, i denotes the imaginary unit and $\bar{z}$ the complex conjugate function of z. Since this is the only position, where the complex unit i appears, there should not be any confusion with the use of i for the electrical current. Also, using the bar for denoting the closure of a set and the complex conjugation should not cause confusions. In what follows, we will write for convenience A_t for $\partial A/\partial t$.

DEFINITION 2.1. *A function $A : [0,T] \to Y(\Omega)$ is said to be a weak solution of the shortened system (2.7), (2.8), if it has the regularity properties $A \in L^2(0,T;Y(\Omega))$, $\sigma A \in C([0,T],V)$, $\sigma A_t \in L^1(0,T;Y(\Omega)')$, fulfills that $t \mapsto \int_{\Omega_2} E(x)\cdot A(x,t)\,dx$ belongs to $H^1(0,T)$, and satisfies the equations*

$$\begin{aligned} &\langle \sigma A_t(t)\,,\,\bar{z}\rangle_{Y(\Omega)',Y(\Omega)} + a_0(A(\cdot,t),\bar{z}) \\ &\quad + R_c^{-1}\left(\int_{\Omega_2} E(x)\cdot A_t(x,t)\,dx\right)\left(\int_{\Omega_2} E(x)\cdot \bar{z}(x)\,dx\right) \\ &= R_c^{-1}\int_{\Omega_2} E(x)\cdot\bar{z}(x)\,dx\,u(t) \quad \forall z \in Y(\Omega), \text{ for a.a. } t \in (0,T), \end{aligned} \tag{2.10}$$

$$A(x,0) = A_0(x) \quad \text{for a.a. } x \in \Omega_{tb}. \tag{2.11}$$

$$\int_{\Omega_2} A(x,0)\cdot E(x)\,dx = \alpha_0. \tag{2.12}$$

3. Definition of optimal control problems and existence of optimal controls.

3.1. Objective functionals and control problems. At $t = 0$, the magnetization process starts with some initial potential A_0 that defines an initial magnetic induction $B_0 := \operatorname{curl} A_0$. The aim of the optimization is to reach the opposite magnetic induction $-B_0 = -\operatorname{curl} A_0$ as fast as possible. Let us write for convenience $B_T := -B_0$.

We cannot expect to (exactly) reach B_T in finite time, hence the time-optimal control problem of reaching B_T in shortest time might not be well posed. To overcome this obstacle, we fix a sufficiently large final time $T > 0$ and aim at minimizing the tracking type functional

$$\begin{aligned} J := \frac{\lambda_T}{2}\int_{\Omega_1} |\operatorname{curl} A(x,T) - B_T(x)|^2\,dx + \frac{\lambda_Q}{2}\iint_{Q_1} |\operatorname{curl} A(x,t) - B_T(x)|^2\,dxdt \\ + \frac{\lambda_u}{2}\int_0^T u(t)^2\,dt. \end{aligned}$$

The first integral of this functional is to approach B_T, the second forces the approximation of B_T to be fast. In the time-optimal control of electrical circuits we have confirmed that this method computes solutions that are very close to time-optimal ones, cf. [3].

This choice of the objective functional inherits some difficulties. For controls $u \in L^2(0,T)$, the regularity of A we are able to prove is not sufficient to define the value $\operatorname{curl} A(T)$. This term is well defined in $L^2(\Omega)^3$ for $u \in H^1(0,T)$. Therefore, we will be able to prove the existence of associated optimal controls only for the choice $\lambda_T = 0$. Numerical computations are based on finite-dimensional approximations of the state equation by finite elements. Here, this obstacle does not appear and we were able to optimize J also for $\lambda_T > 0$.

We also consider the simpler objective functional

$$J_{\text{pot}} := \frac{\lambda_T}{2} \int_{\Omega_1} |A(x,T) - A_T(x)|^2 \, dx + \frac{\lambda_Q}{2} \iint_{Q_1} |A(x,t) - A_Q(x,t)|^2 \, dxdt + \frac{\lambda_u}{2} \int_0^T u(t)^2 \, dt,$$

where $A_T \in L^2(\Omega_1)^3$ and $A_Q \in L^2(Q_1)^3$ are given desired vector fields. This functional evaluates the vector potential A rather than the magnetic induction B. In particular, the choice $A_T(x) = -A_0(x)$ and $A_Q(x,t) = -A_0(x)$ is of interest. This means that, initiating from the vector potential A_0, we want to reach $-A_0$ in short time. This objective functional delivers good results in the practical application but it turned out that by the functional J even better results can be achieved. We consider the optimal control for the functional J_{pot} for comparing these results with the new ones for the curl-functional J.

Let us embed J in a more general form, where vector functions $B_T \in L^2(\Omega)^3$ and $B_Q \in L^2(Q)^3$ are given. We define

$$J(A,u) := \frac{\lambda_T}{2} \int_{\Omega_1} |\operatorname{curl} A(x,T) - B_T(x)|^2 \, dx + \frac{\lambda_Q}{2} \iint_{Q_1} |\operatorname{curl} A(x,t) - B_Q(x,t)|^2 \, dxdt + \frac{\lambda_u}{2} \int_0^T u(t)^2 \, dt,$$

where $\lambda_T \geq 0$ is an optional parameter that will be set to zero in our analysis. In our application to time-optimal switching between magnetic fields, we set

$$B_T(x) = B_Q(x,t) := -\operatorname{curl} A_0(x).$$

Next, we fix the control constraints for our optimal control problems. The control function u must be bounded, i.e.

$$\alpha \leq u(t) \leq \beta \quad \text{for a.a. } t \in [0,T],$$

where real constants $\alpha < \beta$ are given. Hence, the set of admissible controls is defined by

$$U_{ad} := \{u \in L^2(0,T) \,|\, \alpha \leq u(t) \leq \beta \quad \text{for a.a. } t \in [0,T]\}.$$

We discuss two types of optimal control problems. The first optimal control problem has the full system as state equation,

$$\text{(P)} \qquad \min_{u \in U_{ad}} J(A_u, u),$$

where A_u is the first component of the solution vector (A, i) of the full system (2.5).

At this point, this definition is formal, since we do not know if (2.5) admits a solution for control functions u that only belong to $L^2(0,T)$. In view of this, we also discuss an auxiliary control problem for the shortened system as state equation,

$$(\text{P}_{\text{aux}}) \qquad \min_{u \in U_{ad}} J(A_u, u) \qquad \text{with } A_u \text{ subject to (2.7), (2.8).}$$

As numerical example we also deal with a third control problem that is based on the functional J_{pot},

$$(\text{P}_{\text{pot}}) \qquad \min_{u \in U_{ad}} J_{\text{pot}}(A_u, u) \qquad \text{with } A_u \text{ subject to (2.5).}$$

3.2. Existence of optimal controls. The following result follows from Corollary 3.13 in [21]:

LEMMA 3.1 (Well-posedness of the state equations).

(i) For all $u \in L^2(0,T)$, divergence free $A_0 \in L^2(\Omega_1)^3$, and all $\alpha_0 \in \mathbb{R}$, the shortened system (2.7), (2.8) has a unique weak solution $A \in L^2(0,T;Y(\Omega))$ with the following regularity properties: There is a constant $c > 0$ not depending on f and A_0 such that

$$\begin{aligned} &\|A\|_{L^2(0,T;Y(\Omega))} + \|A\|_{C([0,T],L^2(\Omega_1)^3)} + \|\sigma A_t\|_{L^1(0,T;Y(\Omega)')} \\ &\qquad + \Big\| \int_{\Omega_2} A(x,\cdot)\cdot E(x)\,dx \Big\|_{H^1(0,T)} \le c\,(\|u\|_{L^2(0,T)} + \|A_0\|_V). \end{aligned} \tag{3.1}$$

(ii) For all $u \in H^1(0,T)$, divergence free $A_0 \in L^2(\Omega_1)^3$ with $curl\,(\mu^{-1}\,curl\,A_0) \in L^2(\Omega_1)^3$, and $i_0 \in \mathbb{R}$, the full system (2.5) has a unique weak solution $(A,i) \in L^2(0,T;Y(\Omega)) \times H^1[0,T]$, with the regularity properties (3.1). Moreover, A belongs to $H^1(0,T;L^2(\Omega)^3)$ with the additional estimate

$$\|A\|_{H^1(0,T;Y(\Omega))} + \|i\|_{H^1(0,T)} \le c\,(\|u\|_{L^2(0,T)} + \|A_0\|_V).$$

The estimate of $\|A\|_{C([0,T],L^2(\Omega_1)^3)}$ in (3.1) follows from Lemma 3.2 and Corollary 3.8 in [21]. The unique weak solution is divergence free in $\Omega_1 \cup \Omega_2$. Together with the interface condition included in the definition of V, this amounts to a gauging condition for A. This follows from the proof of the existence and uniqueness theorem in [21], where the weak solution is obtained as the limit of divergence free strong solutions.

The continuity estimate in (ii) follows from [21]: The H^1-estimate for A is a consequence of [21], (3.40). Having this estimate, the one for i follows from the very last formula of [21].

By (3.1), the mapping $u \mapsto A_u$ is continuous from $L^2(0,T)$ to the spaces indicated in (3.1). In particular, it is continuous from $L^2(0,T)$ to $L^2(0,T;H(\mathrm{curl}\,,\Omega_1)) \cap C([0,T],L^2(\Omega_1)^3)$, if the restriction $A_u|_{\Omega_1}$ is considered.

The objective functional J is strictly convex and continuous on the space $L^2(0,T;H(\mathrm{curl}\,,\Omega_1)) \times L^2(0,T)$, hence weakly lower semicontinuous. The same holds true for J_{pot} on $C([0,T],L^2(\Omega_1)^3) \times L^2(0,T)$.

LEMMA 3.2 (Existence of optimal controls).

(i) If $A_0 \in L^2(\Omega_1)^3$ is divergence free and $\lambda_T = 0$ holds, then the optimal control problem ($\mathrm{P}_{\mathrm{aux}}$) has a unique optimal control.

(ii) If $A_0 \in L^2(\Omega_1)^3$ satisfies the assumptions of Lemma 3.1, part (ii), then the optimal control problem ($\mathrm{P}_{\mathrm{pot}}$) has a unique optimal control.

Proof. Part (i) of the lemma is a standard conclusion from the lower semicontinuity of the objective functional J. Part (ii) is more delicate, because the state equation (2.5) does possibly not have a solution for all controls u of $L^2(0,T)$. The result was proven in [20] by a detour via the system (2.7), (2.8). □ We were not able to show that also the optimal control problem (P) has an optimal control and had to leave this as an open question. However, in numerical approximations, we solve an approximated version of (P). Since this is a finite-dimensional problem, difficulties with existence of an optimal solution do not appear.

4. Necessary optimality conditions.

4.1. Adjoint calculus. To establish necessary optimality conditions, we first follow a standard step of optimization theory. Since the analysis of ($\mathrm{P}_{\mathrm{aux}}$) is more complete, we discuss the optimality conditions for this problem. We fix $\lambda_T = 0$ for the same reason and mention the case $\lambda_T > 0$ only for completeness in a formal way.

Let us introduce the reduced objective functional

$$\hat{J}(u) := J(A_u, u) = \frac{\lambda_Q}{2} \iint_{Q_1} |\operatorname{curl} A_u(x,t) - B_Q(x,t)|^2 \, dxdt + \frac{\lambda_u}{2} \int_0^T u(t)^2 \, dt.$$

For establishing necessary optimality conditions and also for numerical purposes, we need a simple expression for the derivative $\hat{J}'(u)\, v$, where $v \in L^2(0,T)$ is an arbitrary direction. By the chain rule, we find

$$\hat{J}'(u)\, v = \lambda_Q \int_{Q_1} (\operatorname{curl} A_u - B_Q) \cdot \operatorname{curl} A_v \, dxdt + \lambda_u \int_0^T u\, v \, dt. \tag{4.1}$$

To simplify the first integral in (4.1), we introduce an *adjoint equation*,

$$\left\{ \begin{array}{rcll} -\sigma_0 \dfrac{\partial P}{\partial t} + \operatorname{curl} \mu^{-1} \operatorname{curl} P + \varepsilon\, P &=& \lambda_Q \operatorname{curl} (\operatorname{curl} A_u - B_Q) & \text{in } Q_1 \\ -\dfrac{1}{R_c} \displaystyle\int_{\Omega_2} \frac{\partial P}{\partial t}(\xi,\cdot) \cdot E(\xi)\, d\xi \; E & & & \\ \qquad + \operatorname{curl} \mu^{-1} \operatorname{curl} P - \varepsilon\, P &=& 0 & \text{in } Q_2 \\ P \times \nu &=& 0 & \text{on } \Sigma_T \\ P(x,T) &=& 0 & \text{in } \Omega_1 \\ \displaystyle\int_{\Omega_2} P(x,T) \cdot E(x)\, dx &=& 0. & \end{array} \right. \tag{4.2}$$

In contrast to the optimal control problem ($\mathrm{P}_{\mathrm{pot}}$), where we are able to prove the existence and uniqueness of an adjoint state associated with each control $u \in U_{ad}$, cf. [20], we have to impose some additional assumptions of smoothness for solving the problem of existence of an adjoint state. We were able to prove the following result:

THEOREM 4.1 (Existence of an adjoint state). *Assume that the control u belongs to $H^1(0,T)$, the initial potential A_0 is divergence free and satisfies $curl(\mu^{-1} curl\, A_0) \in L^2(\Omega)^3$, the target B_Q belongs to $L^2(0,T;H(curl\,,\Omega))$ and is divergence free for a.a. $t \in (0,T)$, and that the function μ is constant in Ω_1. Then the adjoint system* (4.2) *has a unique weak solution P that enjoys the same regularity as A that is stated in Lemma 3.1, part (i).*

Proof. Thanks to Theorem 3.14 of [21] and to the assumed higher smoothness of u and A_0, the function A_u has higher regularity, namely

$$A_u \in H^1(0,T;H(\operatorname{curl}\,,\Omega)).$$

This implies

$$\frac{\partial A_u}{\partial t} \in L^2(0,T;H(\operatorname{curl}\,,\Omega)).$$

From the first equation of the system (2.7) in Ω_1 we find that

$$\operatorname{curl}(\mu^{-1}\operatorname{curl} A_u) \in L^2(0,T;L^2(\Omega_1)).$$

Since μ is constant, this is equivalent to $\operatorname{curl}\operatorname{curl} A_u \in L^2(0,T;L^2(\Omega_1))$. In view of the assumption on B_Q, the right-hand side of the first equation of the adjoint system belongs to $L^2(0,T;L^2(\Omega_1))$. Thanks to $\operatorname{div}\operatorname{curl} = 0$, this right-hand side is divergence free. Moreover, the right-hand side of the second equation in this system is a multiple of E, namely zero. Altogether, the assumptions of Theorem 3.11 of [21] for the Maxwell integro-differential equation are fulfilled and we obtain the formulated existence and uniqueness result for P. Notice that the adjoint equation can be transformed by the standard setting $\tau := T - t$ to a forward equation, where the theory of [21] applies. □

REMARK 1. *If $\lambda_T > 0$, then the homogeneous terminal condition for P must be replaced by*

$$\sigma_0\, P(x,T) = \lambda_T\, curl\,(curl\, A_u(x,T) - B_T(x)).$$

This is useful for numerical computations in finite-dimensional approximations of the control system. As we mentioned above, this is not justified by our analysis of the state equation, because the function $curl\,(curl\, A_u(\cdot,T) - B_T(\cdot))$ is not necessarily well defined in $L^2(\Omega_1)^3$.

LEMMA 4.2. *Let $u \in H^1(0,T)$ be a given control for $(\mathrm{P}_{\mathrm{aux}})$ with associated state A_u, $v \in L^2(0,T)$ be an arbitrary direction and denote by A_v the state associated with v subject to the initial condition $A_v(x,0) = 0$ in Ω_1 and $\alpha_0 = 0$.*

Assume that A_0, B_Q, and μ satisfy the assumptions required by Theorem 4.1 . Then there exists a unique weak solution P_u of (4.2) such that

$$\int_{Q_1} (curl\, A_u - B_Q) \cdot curl\, A_v \, dxdt = \int_0^T \left(\int_{\Omega_2} E(x) \cdot P_u(x,t)\, dx \right) v(t)\, dt \tag{4.3}$$

holds for all $v \in L^2(0,T)$.

Proof. Let us assume that v belongs to $H^1(0,T)$. If this does not hold, we select a sequence of functions $v_n \in H^1(0,T)$ converging to v in $L^2(0,T)$ (recalling that $H^1(0,T)$ is dense in $L^2(0,T)$) and prove the desired relation for each v_n. Passing to the limit in (4.3) we get the result for any $v \in L^2(0,T)$. Let us write for short $A := A_v$ and $P := P_u$ to avoid too many repeated indices.

Now, we use P as test function in the weak formulation of the state equation (2.7) and obtain, after adding the two upper parts of this equation,

$$\begin{aligned} \int_0^T \int_\Omega \sigma \frac{\partial A}{\partial t} \cdot P\, dxdt + \frac{1}{R_c} \int_0^T \int_\Omega \int_{\Omega_2} \frac{\partial A}{\partial t}(\xi,t) \cdot E(\xi)\, d\xi\, E(x) \cdot P(x,t)\, dxdt \\ + \int_0^T a_0(A(t),P(t))\, dt = \frac{1}{R_c} \iint_{Q_2} E(x) \cdot P(x,t)\, v(t)\, dxdt. \end{aligned} \tag{4.4}$$

Thanks to our working assumption on v, the derivative $\partial A/\partial t$ is sufficiently smooth so that the first integral in the equation above is well defined. Analogously, we use A as test function in the

adjoint equation (4.2) and obtain

$$
\begin{aligned}
&- \int_0^T \int_\Omega \sigma \frac{\partial P}{\partial t} \cdot A \, dxdt + \int_0^T a_0(A(t), P(t)) \, dt \\
&- \frac{1}{R_c} \int_0^T \int_{\Omega_2} \frac{\partial P}{\partial t}(\xi, t) \cdot E(\xi) \, d\xi \int_{\Omega_2} E(x) \cdot A(x,t) \, dxdt \\
&= \int_0^T \int_{\Omega_1} \lambda_Q \operatorname{curl} (\operatorname{curl} A_u(x,t) - B_Q(x,t)) \cdot A(x,t) \, dxdt. \\
&= \int_0^T \int_{\Omega_1} \lambda_Q \, (\operatorname{curl} A_u(x,t) - B_Q(x,t)) \cdot \operatorname{curl} A(x,t) \, dxdt.
\end{aligned}
$$

In the integrals containing $\partial P/\partial t$, we perform an integration by parts with respect to t and find

$$
\begin{aligned}
&\int_0^T \int_\Omega \sigma \frac{\partial A}{\partial t} \cdot P dxdt + \int_0^T a_0(A(t), P(t)) \, dt \\
&+ \frac{1}{R_c} \int_{\Omega_2} P(\xi, 0) \cdot E(\xi) \, d\xi \int_{\Omega_2} A(x,0) \cdot E(x) \, dx \\
&- \frac{1}{R_c} \int_{\Omega_2} P(\xi, T) \cdot E(\xi) \, d\xi \int_{\Omega_2} A(x,T) \cdot E(x) \, dx \\
&+ \frac{1}{R_c} \int_0^T \int_{\Omega_2} \int_{\Omega_2} \frac{\partial A}{\partial t}(\xi, t) \cdot E(\xi) \, d\xi \, e(x) \cdot P(x,t) \, dxdt \\
&= \int_0^T \int_{\Omega_1} \lambda_Q \, (\operatorname{curl} A_u(x,t) - B_Q(x,t)) \cdot \operatorname{curl} A(x,t) \, dxdt,
\end{aligned}
\tag{4.5}
$$

where we have used that $A(x,0) = 0$ and $P(x,T) = 0$ in Ω_1. Invoking the conditions

$$
\int_{\Omega_2} E(x) \cdot A(x,0) \, dx = 0, \quad \int_{\Omega_2} P(x,T) \cdot E(x) \, dx = 0,
$$

and subtracting the equation (4.5) from (4.4), we deduce

$$
\begin{aligned}
&\int_0^T \int_{\Omega_1} \lambda_Q \, (\operatorname{curl} A_u(x,t) - B_Q(x,t)) \cdot \operatorname{curl} A(x,t) \, dxdt \\
&= \int_{Q_2} E(x) \cdot P(x,t) \, v(t) \, dxdt = \int_0^T \int_{\Omega_2} E(x) \cdot P(x,t) \, v(t) \, dxdt.
\end{aligned}
$$

Returning to the notations $P_u := P$ and $A_v := A$, we verify the desired relation (4.3). ∎

By this result, we obtain the following corollary on the reduced gradient:

COROLLARY 4.3. *For all u in $H^1(0,T)$ and $v \in L^2(0,T)$, the derivative $\hat{J}'(u)$ is given by*

$$
\hat{J}'(u) \, v = \int_0^T \left(\int_{\Omega_2} E(x) \cdot P_u(x,t) \, dx + \lambda_u \, u(t) \right) v(t) \, dt, \tag{4.6}
$$

where P_u is the adjoint state associated with u that is the unique solution to the adjoint equation (4.5).

According to the Riesz theorem, the linear continuous functional $v \mapsto \hat{J}'(u)\, v$ can be represented by a unique element of the underlying Hilbert space $L^2(0,T)$. This is the function standing in brackets under the integral above that is called *reduced gradient*. Identifying $\hat{J}'(u)$ with this function, we can write

$$(\hat{J}'(u))(t) = \int_{\Omega_2} E(x) \cdot P_u(x,t)\, dx + \lambda_u\, u(t).$$

REMARK 2. *To set up a descent method for solving the problem, the restriction to controls of $H^1(0,T)$ is not a real obstacle. For instance, we can work with piecewise linear and continuous functions as controls, which all belong to $H^1(0,T)$. The space $H^1(0,T)$ is dense in $L^2(0,T)$ so that the restriction to $H^1(0,T)$ does not change the optimal value of the problem.*

4.2. Optimality conditions for ($\mathrm{P}_{\mathrm{aux}}$)**.** Let $u^* \in U_{ad}$ be the unique optimal control of ($\mathrm{P}_{\mathrm{aux}}$). By a standard result of optimization theory, $u^\star$ has to satisfy the following variational inequality as basic necessary optimality condition:

$$\hat{J}'(u^*)(u - u^\star) \geq 0 \text{ for all } u \in U_{ad}. \tag{4.7}$$

According to formula (4.1), applied with $v = u - u^*$, this is equivalent to

$$\lambda_Q \int_{Q_1} (\operatorname{curl} A_{u^*} - B_Q) \cdot \operatorname{curl} A_{u-u^*}\, dxdt + \lambda_u \int_0^T u^*(u - u^*)\, dt \geq 0 \quad \forall u \in U_{ad}. \tag{4.8}$$

By linearity, we have $A_{u-u^*} = A_u - A_{u^*}$. Since $A_u(0) = A_{u^*}(0)$ (all state functions have the same initial value A_0), it holds

$$A_{u-u^*}(0) = 0.$$

Therefore, we are in a situation, where Lemma 4.2 can be applied to simplify (4.8) by an adjoint state. However, we have to assume that we even have $u^* \in H^1(0,T)$. Then Lemma 4.2 and Corollary 4.3 yield the following result on necessary optimality conditions:

THEOREM 4.4. *Let the optimal control u^* of problem* ($\mathrm{P}_{\mathrm{aux}}$) *belong to $H^1(0,T)$ and assume that A_0, B_Q, and μ obey the requirements of Theorem 4.1. Then there exists a unique adjoint state function $P^* := P_{u^\star}$, defined as solution of* (4.2)*, where $u^\star$ is inserted for u and the variational inequality*

$$\int_0^T \left(\int_{\Omega_2} E(x) \cdot P^\star(x,t)\, dx + \lambda_u\, u^\star(t) \right) (u(t) - u^\star(t))\, dt \geq 0 \quad \textit{for all } u \in U_{ad} \tag{4.9}$$

is satisfied.

REMARK 3. *We were not able to prove the existence of an adjoint state P_u also for the case, where the control u only belongs to $L^2(0,T)$. Nevertheless, the optimality conditions contain useful information, because this theoretical difficulty does not occur in discretized versions of the problem, where we also can exploit the associated structure.*

For $\lambda_u > 0$, a standard pointwise discussion of the variational inequality (4.9), yields the projection formula

$$u^*(t) = \mathbb{P}_{[\alpha,\beta]}\left(-\frac{1}{\lambda_u}\int_{\Omega_2} E(x)\cdot P^*(x,t)\,dx\right) \quad \text{for a.a. } t\in(0,T), \tag{4.10}$$

where $\mathbb{P}_{[\alpha,\beta]}:\mathbb{R}\to[\alpha,\beta]$ denotes pointwise projection defined by

$$\mathbb{P}_{[\alpha,\beta]}(x) = \max(\alpha,\min(\beta,x)).$$

In the case $\lambda_u = 0$, the variational inequality holds if and only if

$$u^*(t) = \begin{cases} \alpha, & \text{if} \quad \displaystyle\int_{\Omega_2} E(x)\cdot P^*(x,t)\,dx > 0 \\ \beta, & \text{if} \quad \displaystyle\int_{\Omega_2} E(x)\cdot P^*(x,t)\,dx < 0. \end{cases} \tag{4.11}$$

Moreover, we obtain for a.a. t the implication

$$\alpha < u^*(t) < \beta \quad \Rightarrow \quad \int_{\Omega_2} E(x)\cdot P^*(x,t)\,dx = 0. \tag{4.12}$$

These adjoint based necessary optimality conditions were proved under the assumption that the optimal control u^* belongs to $H^1(0,T)$. The assumption was needed to show the existence of the adjoint state. Alternatively, we can just assume that the adjoint P^* associated with u^* exists. Then we are able to deduce the regularity $u^*\in H^1(0,T)$:

COROLLARY 4.5. *Let $u^*\in U_{ad}$ be the optimal control of* ($\mathrm{P_{aux}}$) *and assume that the adjoint equation has a unique associated solution $P^* := P_{u^*}$ with the regularity of A^* formulated in Lemma 3.1, part (ii). Then the optimal control u^* for* ($\mathrm{P_{aux}}$) *belongs to $H^1(0,T)$.*

Proof. Since the adjoint state P^* possesses the regularity of A^*, the function

$$Q^* : t \mapsto \int_{\Omega_2} E(x)\cdot P^*(x,t)\,dx \tag{4.13}$$

belongs to $H^1(0,T)$. The same holds for the function $t\mapsto \mathbb{P}_{[\alpha,\beta]}(Q^*(t))$, because $f\in H^1(0,T)$ implies that also $\max(f(\cdot),\alpha)$ and $\min(f(\cdot),\beta)$ belong to $H^1(0,T)$, cf. Kinderlehrer and Stampacchia [14]. Therefore, also the optimal control

$$u^* = \mathbb{P}_{[\alpha,\beta]}(Q^*(\cdot)) := \min\big(\max\big(\alpha, Q^*(\cdot)\big),\beta\big) \tag{4.14}$$

is a function of $H^1(0,T)$. ∎

Unfortunately, we do not know if we can avoid one of these two assumptions that are needed to establish adjoint based necessary optimality conditions. This difficulty does not appear in the discussion of the simpler objective functional J_{pot}, see [20].

4.3. Optimality conditions for (P). In the last section, we assumed that the optimal control u^* of ($\mathrm{P_{aux}}$) belongs to $H^1(0,T)$. Then by Lemma 3.1 also the associated optimal electrical current i^* enjoys this regularity provided that the associated assumptions on A_0 of Lemma 3.1, (ii) are

satisfied. In this case, the initial value $i^*(0)$ is well defined. Therefore, we are justified to consider the original state equations (2.5) for the pair of states (y, i).

Let us first fix the notion of a weak solution (y, i) for the full system (2.5).

DEFINITION 4.6. *Given $u \in H^1(0,T)$, $i_0 \in \mathbb{R}$ and $A_0 \in L^2(\Omega_1)^3$ with the regularity $curl(\mu^{-1} curl\, A_0) \in L^2(\Omega_1)^3$, we say that (A, i) is a weak solution of the full system(2.5), if $A \in H^1(0,T; H(curl, \Omega))$ obeys the regularity stated in Lemma 3.1, i belongs to $C[0,T]$, the conditions $A(\cdot, 0) = A_0$ and $i(0) = i_0$ are satisfied, the fifth identity of (2.5) is fulfilled for a.a. $t \in (0,T)$, and*

$$\langle \sigma A_t(\cdot,t); \bar{z} \rangle_{Y(\Omega)', Y(\Omega)} + a_0(A(\cdot,t), \bar{z}) = i(t) \int_\Omega E(x) \cdot \bar{z}(x)\, dx \quad \forall z \in Y(\Omega) \tag{4.15}$$

holds for almost all $t \in (0,T)$.

We do not know whether problem (P) has an optimal control in $L^2(0,T)$, because we are not able to assure that to each L^2-control u there exists a unique weak solution (A_u, i_u). Let us assume, however, that problem (P_{aux}) is solvable with controls of $U_{ad} \cap H^1(0,T)$, i.e. we assume that (P_{aux}) has an optimal control in $H^1(0,T)$. Then (P_{aux}) is equivalent to (P) in $U_{ad} \cap H^1(0,T)$.

In the next subsection, we establish necessary optimality conditions for (P) under this assumption.

4.3.1. Optimality system for problem (P). As movitated above, we assume that (P) has an optimal control in $H^1(0,T) \cap U_{ad}$.

THEOREM 4.7. *Assume that (P) has an optimal control in $u^* \in H^1(0,T) \cap U_{ad}$ and let A_0, B_Q, and μ satisfy the assumptions required in Theorem 4.1. Then there exist a unique pair (P^*, Q^*) of adjoint states satisfying the (full) adjoint system*

$$\left\{ \begin{array}{rcll} -\sigma_0 \dfrac{\partial P}{\partial t} + curl\, \mu^{-1}\, curl\, P + \varepsilon\, P &=& \lambda_Q\, curl(curl\, A^* - B_Q) & in \quad Q_1 \\ -\dfrac{1}{R_c} \dfrac{dQ}{dt}(t)\, E + curl\, \mu^{-1}\, curl\, P + \varepsilon\, P &=& 0 & in \quad Q_2 \\ P \times \nu &=& 0 & on \quad \Sigma_T \\ Q(t) &=& \displaystyle\int_{\Omega_2} P(x,t) \cdot E(x)\, dx & in \quad (0,T) \\ \sigma_0\, P(x,T) &=& 0 & in \quad \Omega_1 \\ Q(T) &=& 0 & \end{array} \right. \tag{4.16}$$

such that the variational inequality

$$\int_0^T (Q^*(t) + \lambda_u\, u^*(t)) \Big(u(t) - u^*(t) \Big)\, dt \geq 0 \quad \forall u \in U_{ad} \tag{4.17}$$

is satisfied.

Proof. The result follows immediately from Theorem 4.4 by substituting

$$Q^*(t) := \int_{\Omega_2} P^*(x,t) \cdot E(x)\, dx.$$

□

The function Q^* can be viewed as the Lagrange multiplier associated with the equation

$$\int_{\Omega_2} \frac{\partial A}{\partial t}(x,t) \cdot E(x)\, dx + R_c\, i(t) = u(t).$$

This property can be easily verified by applying a formal Lagrange technique for deriving optimality systems, cf. [23], Section 3.1.

Analogously to the projection formulas (4.10) and (4.14), there holds

$$u^*(t) = \mathbb{P}_{[\alpha,\beta]}(-{\lambda_u}^{-1}\, Q^*(t)) \quad \text{for almost all } t \in [0,T] \tag{4.18}$$

Numerically, it is easier to handle the full system including the electrical current i than to work with the shortened system, where the current is eliminated. In particular, the initial condition $i(0) = i_0$ is easier to handle than the auxiliary initial condition $\int_{\Omega_2} A(x,0) \cdot E(x)\, dx = \alpha_0$, where α_0 has to be chosen in the right way so that the initial condition for i is fulfilled, cf. [21]. We discussed the shortened system and the associated problem ($\mathrm{P}_{\mathrm{aux}}$) mainly for theoretical reasons.

REMARK 4. *We considered the optimal control problems for H^1-controls, i.e.*

$$\min_{u \in U_{ad} \cap H^1(0,T)} \quad J(A_u, u).$$

Numerically it might be helpful to implement such smoother control functions, for instance by a piecewise linear approximation of u. Notice, however, that a projection formula such as (4.10) *does not hold for piecewise linear approximations of u while it is true for an approximation by step functions. Moreover, in finite-dimensional state approximations, all the difficulties related to possibly non existing adjoint states for L^2-controls do not appear, as the approximated problems are finite-dimensional optimization problems. Moreover, the computed optimal controls looked like approximations of H^1-functions. This indicates that our assumption was fulfilled in the numerical examples. We used step functions as numerical approximation of the controls.*

5. Numerical Examples.

5.1. Introduction. To solve the evolution Maxwell equations numerically, we implemented a finite element method with respect to the space variable and the implicit Euler method with fixed step size in time. This generates very large scale linear algebraic equations, because the equations are considered in 3D spatial domains. Moreover, switching in and off the electrical voltage, very steep curves occur right after the switching time. Therefore, very small time steps must be taken in the implicit Euler method and hence a big number of linear algebraic equations must be solved. Altogether, solving the evolution Maxwell system is very time consuming. This causes long computing times for the numerical optimization of the discretized optimal control problem. We report on this issue in our paper [20]. The use of the FE model turned out to be too demanding for the computation of optimal controls. Therefore, we tested methods of model order reduction to shorten the computational times.

We observed that proper orthogonal decomposition (POD) generated low order models that reflect the behavior of the full FE model surprisingly well. The POD reduced systems consist of a small number of ordinary differential equations and can be solved very fast. Therefore, also the associated reduced optimal control problems can be solved in short time. While an optimization

of the full FE model would need running times in the scale of days or weeks, it took us only a few minutes after model reduction by POD. We report on our associated experience below.

We show numerical examples for a simplified academic geometry that is explained with all details so that the reader is able to check our numerical results by own calculations. Moreover, we present results for an industrial DN50 sensor. In all computational examples, a standard conjugate gradient combined with projected gradient method was applied.

5.2. Model reduction by POD.

5.2.1. Introduction. We give here a short account on POD, a standard method of model order reduction. In the context of optimal control theory for PDEs, we refer to Kunisch and Volkwein [17], [18], Afanasiev and Hinze [1], or Volkwein [24] and to the references cited therein. There is no guarantee that this method generates reliable and precise approximations for any type of evolution equations. For instance, it may fail in the application to Navier-Stokes equations in the case of high Reynolds numbers, where turbulent flows arise. However, we have good experience with linear and nonlinear versions of the heat equations.

Due to certain similarities in the behavior of magnetization processes with heat conduction, we expected that POD might fit to our application, too. Fortunately enough, we were right, POD was extremely efficient as we shall demonstrate out below.

5.2.2. A short sketch of POD. The main idea behind POD is the following: Let $0 \le t_1 < \ldots < t_n \le T$ be an equidistant partition of the time interval $[0,T]$ and compute snapshots $A(t_i)$, $i = 1,\ldots,n$, of the solution A to (2.5). Since this is numerically done by an FE approximation, we have the correspondence

$$A(t_i) \sim A_i \in \mathbb{R}^{n_{\mathrm{FEM}}}, \quad i = 1,\ldots,n,$$

where n_{FEM} is the dimension of the finite element space. For a given natural number r, we determine orthonormal vectors $p_1,\ldots,p_r \in \mathbb{R}^{n_{\mathrm{FEM}}}$ with $r \le d = \dim \operatorname{span}\{A_1,\ldots,A_n\} \le n_{\mathrm{FEM}}$ that approximate the system $\{A_1,\ldots,A_n\}$ best in the following sense:

$$\sum_{i=1}^{n} \Big| A_i - \sum_{k=1}^{r} \langle A_i, p_k\rangle p_k \Big|^2 = \min_{v_1,\ldots,v_r} \sum_{i=1}^{n} \Big| A_i - \sum_{k=1}^{r} \langle A_i, v_k\rangle \; v_k \Big|^2 \tag{5.1a}$$

subject to

$$\langle v_i, v_j\rangle = \delta_{ij} \quad \forall\, i,j \in \{1,\ldots,r\}. \tag{5.1b}$$

Here, $|\cdot|$ and $\langle\cdot,\cdot\rangle$ denote the Euclidean norm and the associated inner product, respectively. Problem (5.1) can be transformed into an equivalent maximization problem, namely

$$\max_{v_1,\ldots,v_r} \sum_{i=1}^{n} \sum_{k=1}^{r} \langle A_i, v_k\rangle^2$$

subject to

$$\langle v_i, v_j\rangle = \delta_{ij} \quad \forall\, i,j \in \{1,\ldots,r\}.$$

By the Lagrange principle, one obtains the following necessary and sufficient optimality condition for the solution p:

$$\sum_{k=1}^{n} \langle A_k, p_i \rangle \, A_k = \lambda_i \, p_i \qquad \forall \; i \in \{1, \ldots, r\}$$
$$\langle p_i, p_j \rangle = \delta_{ij} \qquad \forall \; i, j \in \{1, \ldots, r\}.$$

The theory of singular value problems ensures the existence of a solution to this problem.

The selection of r depends on the decay of the singular values σ_i of the matrix $Y := [A_1, \ldots, A_n]$ of the snapshots. Only those singular values are selected that are sufficiently large. Then the distance between the collection of snapshots $A(t_i)$ and the approximation by the first r eigensolutions can be estimated in the norm of an appropriate space X, say $X = L^2(\Omega)^3$ equipped with the inner product $(\cdot\,, \cdot)$, by

$$\sum_{i=1}^{n} \| A(t_i) - \sum_{k=1}^{r} (A(t_i), p_k) \; p_k \|^2 \leq \sum_{k=r+1}^{d} \sigma_k^2,$$

where the p_k are re-interpreted as functions of the FE space, cf. Hinze and Volkwein [10]. This estimate indicates how large the expected error is, if the r first eigenelements are taken.

POD has a theoretical drawback. This estimate is not uniform with respect to the control u that was taken to establish the snapshots. Therefore, the optimal control of the POD reduced system might theoretically lead to a wrong optimal control. We did not observe such problems. In particular, the desired final state (of the full model) was well approximated at $t = T$. This indicates that POD leads to reasonable results. We will comment on this in Section 5.3.2.

Let us now briefly sketch the implementation of the POD method.

POD Algorithm.

1. Calculate the matrix of snapshots $Y := [A_1, \ldots, A_n] \in \mathbb{R}^{n_{\text{FEM}} \times n}$.

2. Solve one of the following eigenvalue problems to find the singular values σ_i:
   - If $n_{\text{FEM}} \gg n$, then solve
     $$Y^T Y v_i = \sigma_i^2 \, v_i \quad \text{for } \; i = 1, \ldots, d;$$
     define $p_i := \frac{1}{\sigma_i} Y \, v_i$.
   - If not, then solve the eigenvalue problem
     $$Y Y^T p_i = \sigma_i^2 \, p_i \quad \text{for } \; i = 1, \ldots, d.$$

3. Choose the r largest eigenvalues; w.l.o.g. let $\sigma_1^2 \geq \ldots \geq \sigma_r^2$. The set of the corresponding vectors $\{p_1, \ldots, p_r\}$ build the new POD-basis with rank r.

4. Use $\{p_1, \ldots, p_r\}$ as new Galerkin basis and apply the Galerkin method with that basis. Compute the associated mass and stiffness matrices and establish the reduced problem.

   We do not discuss the details of this step and refer to the references on the application of the POD method cited above.

5.3. Computational examples of optimal control.

5.3.1. Solution of ($\mathbf{P}_{\mathrm{pot}}$) for the simplified geometry – A-optimization. In this subsection, we consider an example for the functional J_{pot} and the geometry "tube with slit", where the vector field A appears in the objective functional but not $B = \operatorname{curl} A$. Let us refer to this problem as "A-optimization". Here, we have a complete theory of first-order necessary optimality conditions, see [20].

We concentrate here on the tube with slit. Without slit, the principal form of the optimal controls is similar to the setting with slit. We will discuss the influence of the slit in the next subsection, see also Fig. 5.3.

EXAMPLE 2. *We consider the geometry introduced in Example 1 for the following data:*

- *PDE data:*

$$\mu_r = 400, \quad \sigma = 10^6 S/m, \quad R_c = 40\,\Omega,$$
$$N = 1600, \quad |\omega_c| = 0.005 \cdot 0.040 m^2, \quad T = 0.08\,s.$$

  Here, μ_r is the dimensionless relative permeability in the tube. It holds $\mu = \mu_0\,\mu_r$, where $\mu_0 = 4\,\pi 10^{-7}\,H/m$ is the permeability of the vacuum. Outside the tube, we have set $\mu_r = 1$.
- *Bounds and weights:*

$$\lambda_Q = 10^{12}, \quad \alpha = -30, \quad \beta = 30.$$

  For λ_u, we will test a variety of values.

  Since we have set $\lambda_T = 0$, only the ratio of λ_Q and λ_u is relevant for the optimization so that one of the two parameters might be set to one. This is indeed the standard setting in quadratic tracking type funtionals with regularization term. While this is true from an analytic point of view, in the numerical calculations both values have their own right. This is due to possible cancellation of digits. Therefore, we work with λ_Q and λ_u together.
- *Initial state: For A_0, we select a constant vector given by the stationary solution of (2.5) with control $u(t) \equiv i_0 \cdot R_c = 4\,V$.*
- *Numerical solution of the FE system: The evolution Maxwell equation was solved by an elliptic regularization with the operator*

$$u \mapsto curl\,\mu^{-1}\,curl\,u + \varepsilon\,u$$

  and $\varepsilon = 100$. As finite elements, we applied H-curl elements with degree $p = 2$ that obey the associated Dirichlet boundary conditions at $\partial\Omega$. For the Crank-Nicolson method in time, the weight 0.5 and the time step size $\tau = 10^{-5}$ were taken.

Computing the optimal control for the full system is a very time consuming task. Therefore, we investigated the application of model reduction by POD.

The decay of the eigenvalues $\lambda_i := \sigma_i^2$ of $Y^\top Y$ is presented in Fig. 5.1. It turns out that only the first 5 POD modes are essential for the solution. Therefore, a POD Galerkin basis of dimension 5 should be sufficient to establish the reduced control system. This is definitely true for the state function associated with the control that was selected to compute the snapshots. For this, we used a step function like the one shown in Fig. 5.6. We knew from former calculations with the full system that the optimal controls have also the form close to a step function. Therefore, we can

expect that the solutions to the reduced system also well approximate those of the full system that belong to controls out of a certain neighborhood of this control function.

Encouraged by this excellent performance of POD, we determined (sub)optimal controls by solving the POD reduced optimal control problem. We solved ($P_{\rm pot}$) for the values $\lambda_u = 10^n,\ n = 3, \ldots, 8$. The associated POD-optimal control functions are presented in Fig. 5.1. The larger λ_u is, the smaller is the L^2-norm of the optimal control. This is nicely reflected by Fig. 5.1 that shows a monotone sequence of controls. The largest one belongs to $\lambda_u = 1000$ and the smallest to $\lambda_u = 10^8$. Notice that we have taken $\lambda_Q = 10^{12}$. Therefore, for the standard choice $\lambda_Q = 1$, our sequence of λ_u would be equivalent to the selection $\lambda_u = 10^{-9}, \ldots, 10^{-4}$.

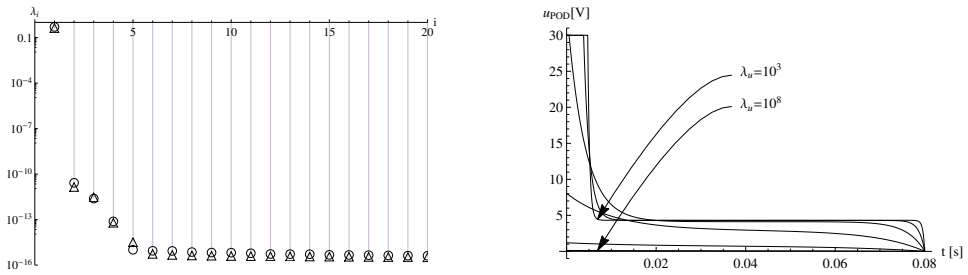

FIG. 5.1. *Example 2, A-optimization: Singular values of Y – circles without slit, triangles with slit (left) and POD optimal optimal controls u_{POD} for problem ($P_{\rm pot}$), geometry with slit, with $\lambda_u = 10^3, \ldots, 10^8$ (right).*

Thanks to formula (4.10), the optimal control u^* must satisfy the equation

$$u^*(t) = \mathbb{P}_{[\alpha,\beta]}\{-\lambda_u^{-1} Q^*(t)\},$$

where Q^* is obtained from (4.13). An analogous formula holds true for the suboptimal control that is optimal for the POD reduced system. Here we write $Q_{\rm POD}$ instead of Q^*. We define accordingly

$$q(t) := \lambda_u^{-1} Q_{\rm POD}(t)$$

and should have $u_{\rm POD}(t) = \mathbb{P}_{[\alpha,\beta]}\{-q(t)\}$. In figure 5.2 we can see that the solution $u_{\rm POD}$ satisfies the optimality test quite well for different selections of λ_u.

5.3.2. Solution of (P) for the simplified geometry - B-optimization. Let us compare the optimal solutions of the last example with optimal solutions of (P), where the curl A is to be optimized, i.e. we are interested in an optimal magnetic field $B = \operatorname{curl} A$; we refer to this setting as "B-optimization". We solved (P) for various values of λ_u in the tube with and without slit. In all cases, the numerical optimization of the POD reduced problems by the projected conjugate gradient method combined with projected gradient steps did not cause any troubles. Some of our results are displayed in Fig. 5.3. Here, we compare optimal controls of ($P_{\rm pot}$) and (P) for selected values of λ_u and for the tube with and without slit.

For the regularization parameter $\lambda_u = 100$, the norm $\|B(T) - B_Q\|_{L^2(\Omega)^3}$ of the reduced state B associated to the optimal control u_{POD} was about 0.0025. Notice that the objective functional measures the difference of B to B_Q in the whole interval of time. Moreover, it contains the regularization term weighted by λ_u.

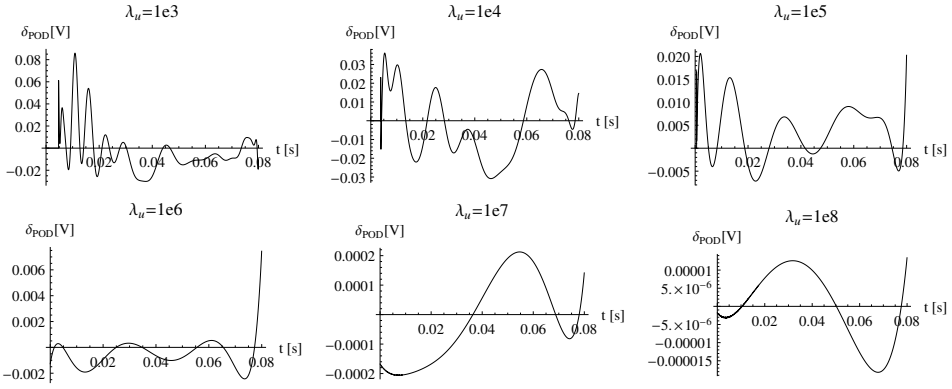

FIG. 5.2. *Example 2, A-optimization: Optimality test* $\delta_{POD} := u_{\mathrm{POD}}(t) - \mathbb{P}_{[\alpha,\beta]}\{-q(t)\}$ *for the optimal controls displayed in Fig. 5.1 for different* λ_u.

In the geometry with slit, the optimal solution can be achieved by smaller controls, i.e. less energy is needed. The reason is the following: In the domain with slit, only smaller eddy currents can develop. Therefore, magnetic fields can be built with less energy.

5.3.3. Optimal control for an industrial sensor. In this example, a real industrial DN50 sensor is considered. The FE mesh, presented in Fig. 5.4, generates 109 282 elements and has 1 054 050 degrees of freedom. To achieve at least a moderate precision, the state equation was solved with only 200 time steps. For a time horizon of $T = 40\,ms$, this amounts to time steps of length $2 \cdot 10^{-4}\,s$. Under this discretization, one solve of the state equation by the FE code NGSOLVE took 5.2 hours. In each iteration of the gradient method, we have to solve the state equation and the adjoint equation, hence 10.4 hours are needed for each iteration. To achieve an acceptable precision, some hundred gradient steps must be performed, say only 100. In this case, the projected gradient method would take more than 43 days of CPU time. It is clear that here the optimization of the full model is fairly useless. However, an optimization of the POD reduced model was very efficient.

Also for this complicated geometry of the DN50 sensor, we observe rapid decay of the singular values of the snapshot matrix Y, cf. Fig. 5.5. For a fixed step function as control, the difference between the solution of the reduced system with 8 basis functions and the solution of the full FE system is shown for the industrial DN50 sensor in Figure 5.6. Step functions of this type are close to the optimum, as computations for the full system by Altmann [2] show. In the right upper picture of Fig. 5.6, the associated currents i_c are displayed that are obtained by the full FE model and the POD reduced model. Both currents show perfect graphical coincidence. The difference between both currents is shown in the lower figures.

The POD reduced state equation was easily solvable by Mathematica. The CPU time for one solve of the reduced state equation took only a few milliseconds instead of 5.2h for the full system. By this tremendous savings, the optimization of the whole system was possible within a few minutes.

EXAMPLE 3. *The industrial DN50 sensor was optimized with the following data:*

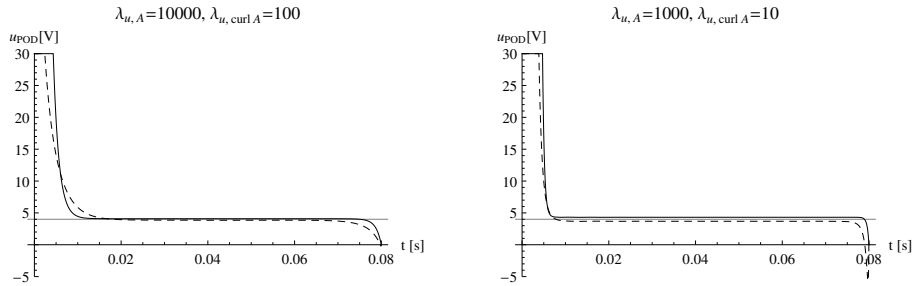

(a) Example 2, comparison of A- and B-optimization: Solutions to ($\mathrm{P_{pot}}$) (thin line) and (P) (dashed line). Left hand side geometry without slit, right hand side geometry with slit.

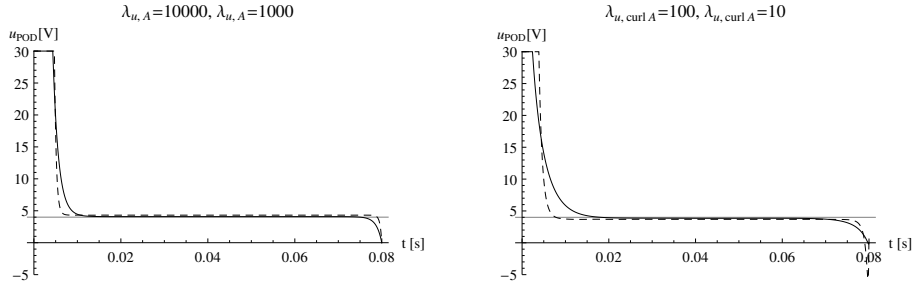

(b) Example 2, comparison of the geometries without slit (thin line) and with slit (dashed line). Left hand side: Problem ($\mathrm{P_{pot}}$), i.e. A-optimization; right hand side: Problem (P), i.e. B-optimization.

FIG. 5.3. *Comparison of solutions to (P) and (P_{pot}) for the tube with and without slit.*

Number of elements:	*109'282*
Degrees of freedom:	*1'054'050*
Total time:	$T = 40ms$
Time stepsize	$dt = 10^{-6}s$
Number of time steps:	*40'000*
Number of POD basis functions:	*8*
Bounds:	$\alpha = -50,\ \beta = 50$

It took us a few seconds of CPU time for solving the optimization problem of Example 3.

The principal form of the optimal controls of the reduced system is very similar to the ones obtained with the simplified geometry for (P) and ($\mathrm{P_{pot}}$). Therefore, we do not display them. Instead, we present here an optimal control for the parameter $\lambda_u = 0$. In this case, the suboptimal control u_{POD} must obey the relations according to (4.11) and (4.12) adapted to the model reduced case. In particular, we must have

$$\begin{aligned} \alpha < u_{\mathrm{POD}}(t) < \beta \quad &\Rightarrow \qquad q(t) = 0, \\ Q_{\mathrm{POD}}(t) < 0 \quad &\Rightarrow \qquad u_{\mathrm{POD}}(t) = \beta. \end{aligned} \tag{5.3}$$

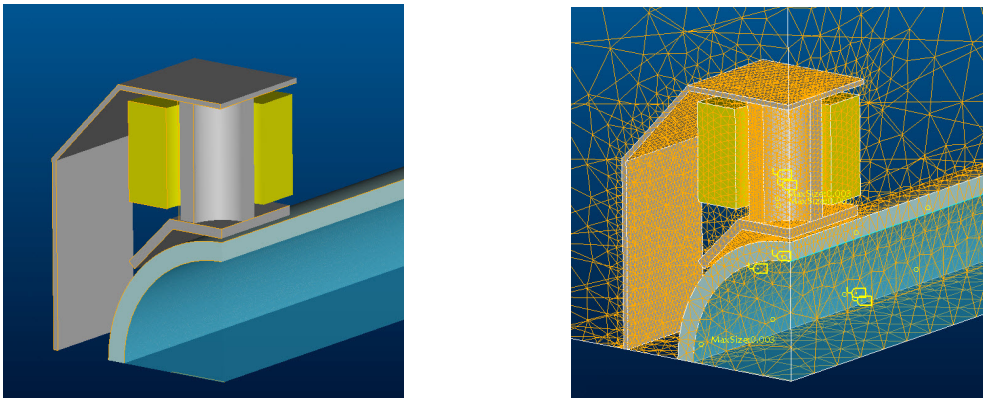

FIG. 5.4. *Example 3: Industrial DN50 Sensor (left) and associated FE grid (right).*

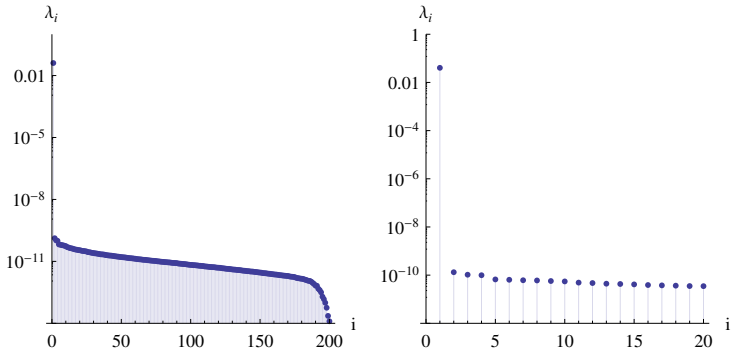

FIG. 5.5. *Example 3: Singular values* $\sigma_i^2 =: \lambda_i$ *of the snapshot matrix* Y *for the DN50 Sensor*

We take this relation as a test of optimality for the control. The optimal control is displayed in Fig. 5.7. It obeys the optimality test (5.3) very well.

The optimal controls for the problems (P) and ($\mathrm{P}_{\mathrm{pot}}$) have the same main structure. Therefore, the question arises if the solutions of the simpler optimal control problem ($\mathrm{P}_{\mathrm{pot}}$) are sufficiently useful so that the more complicated B-optimization is not needed. An answer comes by inspecting Fig. 5.8 that shows the functions $t \mapsto \|\mathrm{curl}\, A(t)\|_{L^2(\Omega)^3}$ for ($\mathrm{P}_{\mathrm{pot}}$) and (P) over a few switching periods. In contrast to the A-optimization in ($\mathrm{P}_{\mathrm{pot}}$), the function $t \mapsto \|\mathrm{curl}\, A(t)\|$ has much smaller maxima for the B-optimization. Moreover, $\|B(t)\| = \|\mathrm{curl}\, A(t)\|$ is less oscillating for the B-optimization. From the viewpoint of flow measurement, this should be preferred.

An interesting effect can be observed from the behavior of the associated optimal electrical currents in Fig. 5.9. As we pointed out in the introduction of our paper, we are interested in switching between constant magnetic fields B in short time. This does not mean that the generated electrical current is as close as possible to a step function. The electrical current associated with the optimal magnetic field of problem (P) is shown in the right-hand side of Fig. 5.9. It is not a step function while the optimal current for ($\mathrm{P}_{\mathrm{pot}}$) is almost one (left-hand side of Fig. 5.9).

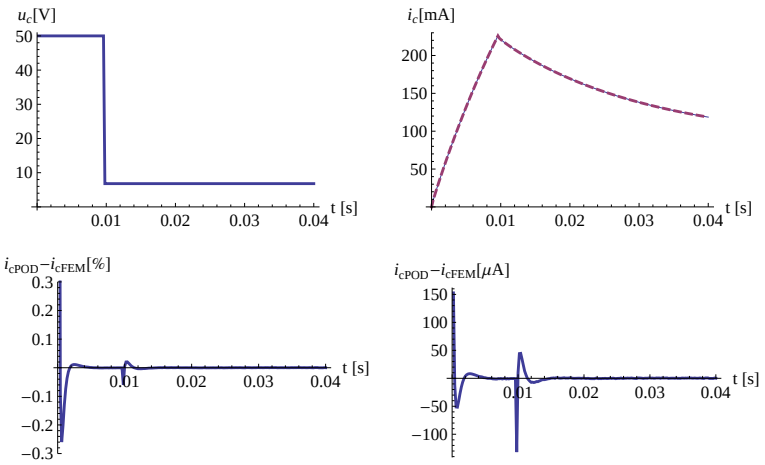

FIG. 5.6. *Example 3: Comparison of FE and POD solution for the DN50 Sensor associated with a step function u*

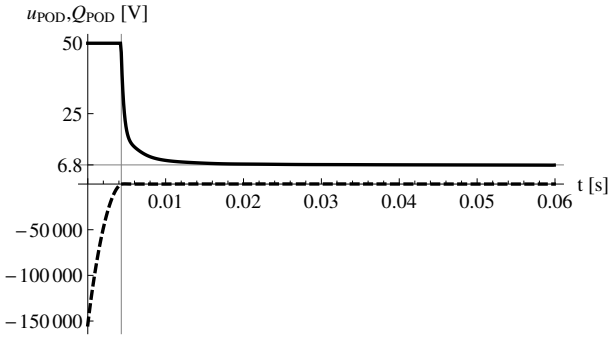

FIG. 5.7. *Example 3, B-optimization for* $\lambda_u = 0$ *and* $\lambda_Q = 1e12$*: Suboptimal control* u_{POD} *(thick line); adjoint function* Q_{POD} *(dashed line).*

REFERENCES

[1] K. Afanasiev and M. Hinze. Adaptive control of a wake flow using proper orthogonal decomposition. In *Shape Optimization & Optimal Design*, volume 216 of *Lect. Notes in Pure and Appl. Math.*, pages 317–332. Marcel Dekker, 2001.

[2] K. Altmann. *Numerische Verfahren der Optimalsteuerung von Magnetfeldern.* Phd thesis, Technical University of Berlin, 2013.

[3] K. Altmann, S. Stingelin, and F. Tröltzsch. On some optimal control problems for electric circuits. *International Journal of Circuit theory*, 2013, doi: 10.1002/cta.1889.

[4] F. Bachinger, U. Langer, and J. Schöberl. Numerical analysis of nonlinear multiharmonic eddy current problems. *Numer. Math.*, 100(4):593–616, 2005.

[5] G. Bärwolff and M. Hinze. Optimization of semiconductor melts. *ZAMM Z. Angew. Math. Mech.*, 86(6):423–437, 2006.

[6] P.E. Druet, O. Klein, J. Sprekels, F. Tröltzsch, and I. Yousept. Optimal control of three-dimensional state-constrained induction heating problems with nonlocal radiation effects. *SIAM J. Control Optim.*, 49(4):1707–1736, 2011.

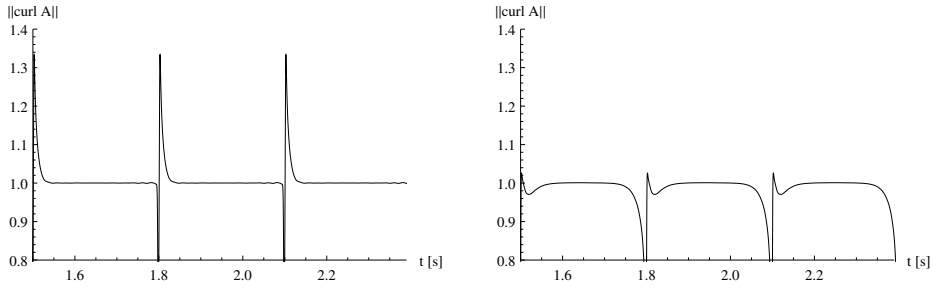

FIG. 5.8. *Example 3: Oscillations of* $t \mapsto \|curl\, A(t)\|_{L^2(\Omega)^3}$ *for A-optimization (left) and B-optimization (right).*

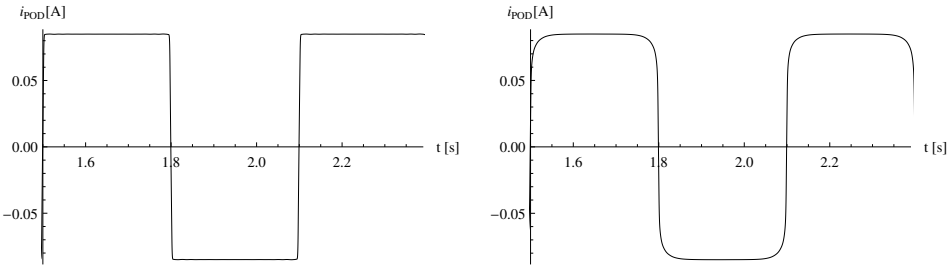

FIG. 5.9. *Example 3: Optimal currents for A-optimization (left) and B-optimization (right)*

[7] R. Griesse and K. Kunisch. Optimal control for a stationary MHD system in velocity-current formulation. *SIAM J. Control Optim.*, 45(5):1822–1845, 2006.

[8] M. Gunzburger and C. Trenchea. Analysis and discretization of an optimal control problem for the time-periodic MHD equations. *J. Math. Anal. Appl.*, 308(2):440–466, 2005.

[9] M. Hinze. Control of weakly conductive fluids by near wall Lorentz forces. *GAMM-Mitt.*, 30(1):149–158, 2007.

[10] M. Hinze and S. Volkwein. Proper orthogonal decomposition surrogate models for nonlinear dynamical systems: Error estimates and suboptimal control. In *Dimension reduction of large-scale systems*, volume 45 of *Lect. Notes Comput. Sci. Eng.*, pages 261–306, Berlin, 2005. Springer.

[11] D. Hömberg and J. Sokołowski. Optimal shape design of inductor coils for surface hardening. *Numer. Funct. Anal. Optim.*, 42:1087–1117, 2003.

[12] L. S. Hou and A. J. Meir. Boundary optimal control of MHD flows. *Appl. Math. Optim.*, 32(2):143–162, 1995.

[13] L. S. Hou and S. S. Ravindran. Computations of boundary optimal control problems for an electrically conducting fluid. *J. Comput. Phys.*, 128(2):319–330, 1996.

[14] D. Kinderlehrer and G. Stampacchia. *An Introduction to Variational Inequalities and their Applications.* Academic Press, New York, 1980.

[15] M. Kolmbauer. *The multiharmonic finite element and boundary element method for simulation and control of eddy current problems.* Phd thesis, 2012.

[16] M. Kolmbauer and U. Langer. A Robust Preconditioned MinRes Solver for Distributed Time-Periodic Eddy Current Optimal Control Problems. *SIAM J. Sci. Comput.*, 34(6):B785–B809, 2012.

[17] K. Kunisch and S. Volkwein. Galerkin proper orthogonal decomposition methods for parabolic problems. *Numer. Math.*, 90(1):117–148, 2001.

[18] K. Kunisch and S. Volkwein. Galerkin proper orthogonal decomposition methods for a general equation in fluid dynamics. *SIAM J. Numerical Analysis*, 40:492–515, 2002.

[19] C. Meyer, P. Philip, and F. Tröltzsch. Optimal control of a semilinear PDE with nonlocal radiation interface conditions. *SIAM J. Control Optimization*, 45:699–721, 2006.

[20] S. Nicaise, S. Stingelin, and F. Tröltzsch. On two optimal control problems for magnetic fields. *In preparation*, 2013.
[21] S. Nicaise and F. Tröltzsch. A coupled Maxwell integrodifferential model for magnetization processes. *Mathematische Nachrichten*, 2013.
[22] S. S. Ravindran. Real-time computational algorithm for optimal control of an MHD flow system. *SIAM J. Sci. Comput.*, 26(4):1369–1388 (electronic), 2005.
[23] F. Tröltzsch. *Optimal Control of Partial Differential Equations. Theory, Methods and Applications*, volume 112. American Math. Society, Providence, 2010.
[24] S. Volkwein. Model reduction using proper orthogonal decomposition. Lecture notes, Institute of Mathematics and Scientific Computing, University of Graz, 2007.
[25] I. Yousept. Optimal control of Maxwell's equations with regularized state constraints. *Comput. Optim. Appl.*, 52(2):559–581, 2012.
[26] I. Yousept and F. Tröltzsch. PDE-constrained optimization of time-dependent 3d electromagnetic induction heating by alternating voltages. *ESAIM M2AN*, 46:709–729, 2012.